IOPscience iopscience.iop.org

Home Search Collections Journals About Contact us My IOPscience

The growth mechanism and morphology of hydrothermally grown oxide compounds: fractal approach

This article has been downloaded from IOPscience. Please scroll down to see the full text article.

2004 J. Phys.: Condens. Matter 16 S1313

(http://iopscience.iop.org/0953-8984/16/14/044)

View the table of contents for this issue, or go to the journal homepage for more

Download details:
IP Address: 129.252.86.83
The article was downloaded on 27/05/2010 at 14:21

Please note that terms and conditions apply.

INSTITUTE OF PHYSICS PUBLISHING JOURNAL OF PHYSICS: CONDENSED MATTER

J. Phys.: Condens. Matter **16** (2004) S1313–S1324 PII: S0953-8984(04)74996-6

The growth mechanism and morphology of hydrothermally grown oxide compounds: fractal approach

L N Demianets and A K Ivanov-Schitz

Institute of Crystallography, RAS, Leninsky Prospekt 59, 119333, Moscow, Russia

E-mail: demianets@ns.crys.ras.ru

Received 22 January 2004
Published 26 March 2004
Online at stacks.iop.org/JPhysCM/16/S1313
DOI: 10.1088/0953-8984/16/14/044

Abstract

Single crystals of Fe_2O_3 (haematite), $Be_3Al_2Si_6O_{18}$ (beryl) have been grown on seeds from hydrothermal solutions. Optical microscopy and AFM have been used for the study of the growth morphology of atomically smooth faces of single crystals as well as of the surfaces growing in accordance with the regeneration growth mechanism. Profiles of the crystallization front have been obtained for different directions of crystallization. Their analysis has shown that the growth morphology may be numerically characterized using the elements of fractal theory. The calculated values of the fractal dimensions are different for layer-by-layer growth and regeneration growth. For beryl single crystals, fractal analysis of the growth surface has been carried out and numerical fractal characteristics have been obtained using the area–perimeter method.

(Some figures in this article are in colour only in the electronic version)

1. Introduction

Crystal growth on substrates seeds is of special interest as a specific case of directed crystallization. The regeneration of crystal takes place on the seed. This is a process of reconstruction of the characteristic crystallographic form or the transformation of an arbitrary shape into a faceted form which is stable under the growth conditions.

Most hydrothermally grown crystals demonstrate very low growth rates of singular faces if the growth occurs on a substrate with the same orientation, and it is necessary to use another way to grow bulk crystals. One of the ways is to use nonsingular surfaces as substrate surfaces. Such surfaces are inclined from the right crystallographic orientation by some angle and the rate of regeneration of such surfaces can be several orders higher than growth rates of singular faces [1–3]. Now it is obvious that crystal growth of complicated compounds takes place due

 © 2004 IOP Publishing Ltd Printed in the UK

Table 1. Growth conditions and characteristics of haematite and beryl single crystals.

Composition	Fe_2O_3	$Be_3Al_2Si_6O_{18}$:Cr^{3+}
Space group	$R\bar{3}c$	$P6/mmc$
Unit cell parameters (Å)	$a = 5.035$, $c = 13.749$	$a = 9.223$, $c = 9.211$
Solvent	NaOH, Na_2CO_3	Acidic solvent
Growth temperature (°C)	390–425	600
Pressure (atm)	800–1200	2500–3000
Seed orientation	(0001), $(11\bar{2}0)$, $(10\bar{1}0)$	Inclination 5°–10° from the surfaces $\{11\bar{2}1\}$, $\{11\bar{2}2\}$
Growth rate (mm/day)	0.02–0.06	0.2–0.25
Habit-forming simple crystallographic forms	Hexagonal prism of the second kind $\{11\bar{2}0\}$; Pinacoid {0001}; Negative rhombohedron $\{01\bar{1}4\}$; Positive rhombohedron $\{10\bar{1}2\}$	Prism $\{10\bar{1}0\}$, Prism $\{11\bar{2}0\}$, Bipyramid of the second kind $\{11\bar{2}1\}$, Bipyramid of the first kind $\{10\bar{1}2\}$, Pinacoid $\{000\bar{1}\}$

to attaching on the growing surface not individual atoms (ions), but some building units which are characteristic for those systems and may consist of different numbers of atoms.

New data on crystal growth have initiated the search for new ways of describing the growth process and the crystal as its final result. We suggest a new approach for the analysis of crystal growth based on the use of the elements of fractal theory.

When growth takes place on plane-parallel substrate seeds, the crystallization front is represented by the surface of the growing face of the single crystal. To analyse the crystallization front one usually uses a traditional description of the object with the help of geometrical figures (lines, segments, polygons, etc); the topological dimension of such objects is equal to the metric dimension.

Mandelbrot [4] was the first to show that a lot of shapes which were described before only at a general descriptive level may be analysed in the framework of a fractal approach with quantitative evaluations. Nowadays, elements of fractal theory are widely used for the description of various phenomena and processes in chemistry, physics, and biology [5–8]. A similar approach seems to be very promising in the analysis of the growth mechanism in the process of crystal regeneration when the formation of the crystal final shape passes through several stages (appearance–development–disappearance of the faces of simple crystallographic forms, depending on face characteristics and growth conditions).

2. Objects and methods of investigation

We describe here the results of a growth and morphology investigation for two oxygen-containing compounds; they are an oxide Fe_2O_3 (haematite) and a complicated ring silicate $Be_3Al_2Si_6O_{18}$ (beryl). These compounds are grown under hydrothermal conditions in strongly alkali or strongly acidic solutions (table 1) and demonstrate the specific features of regeneration processes.

The single crystals have been studied by the methods of x-ray diffraction, etching, and optical and atomic force microscopies. X-ray analysis was performed using the diffractometer Rigaku D-Max 1500, with Cu Kα radiation. An optical microscope 'Neophot 32' was used for

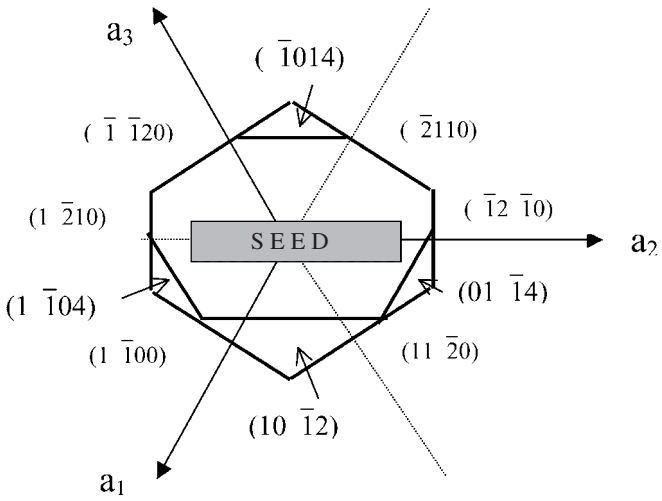

Figure 1. Haematite. Simple crystallographic forms of grown crystal. Projection onto the (0001) plane.

obtaining surface morphology images of as-grown crystals. The pictures of the crystal surfaces were obtained using the scanning atomic force microscope Solver P47 HT-MOT (Moscow) in a tapping mode (Si cantilevers, NSC 11/15, MikroMasch production) with the following characteristics: radius of curvature less than 10 nm; tip height 15–20 μm; full tip cone angle less than 20°; reflecting side covered by Al. The cantilever length and width were 90 ± 5 and 60 ± 3 μm respectively; the cantilever thickness was 2 μm; the resonant frequency was ∼315 kHz; the force constant was ∼48 N m^{-1}.

The analysis of the sets of experimental AFM data gives the following information:

(1) $R_{\max}$ is the swing of heights or the difference between the maximal heights and maximal depths of the peaks:

$$R_{\max} = |Z_{\max}| - |Z_{\min}|.$$

This parameter is used for general evaluation of the degree of relief non-uniformity.

(2) R_{mean} is a mean value of the heights for all points:

$$R_{\text{mean}} = \frac{1}{N_x N_y} \sum_{i=1}^{N_x} \sum_{j=1}^{N_y} |Z|.$$

(3) R_{a} is a mean normalized roughness. It determines the roughness of the surface as an arithmetical mean value. For symmetric relief one can use the abscissa of the mode of the height distributions. For a rectangular mass, $N_x \times N_y$,

$$R_{\text{a}} = \frac{1}{N_x N_y} \sum_{i=1}^{N_x} \sum_{j=1}^{N_y} |Z|.$$

3. Results and discussion

3.1. Crystal habit

Haematite Fe_2O_3. Spontaneous crystallization of haematite in hydrothermal alkaline solutions results in the formation of a plate habit which is created by the following simple

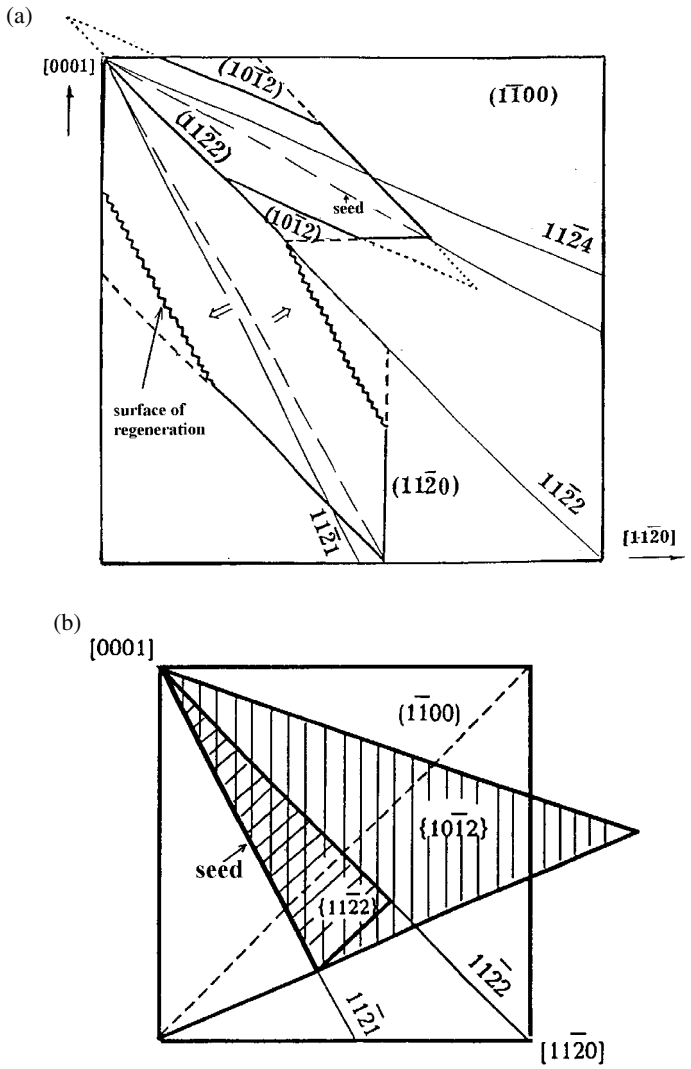

Figure 2. Beryl. (a) Simple crystallographic forms of grown crystals. Projection onto the (1$\bar{1}$00) plane. (b) Regeneration pyramids {10$\bar{1}$2) and {11$\bar{2}$2}. Projection onto the (1$\bar{1}$00) plane.

crystallographic forms: pinacoid {0001), positive rhombohedron {10$\bar{1}$2}, hexagonal bipyramid {11$\bar{2}$3}. When seeds parallel to the prism faces were used, the crystal habit was formed by the faces of a negative rhombohedron {01$\bar{1}$4}, a positive rhombohedron {10$\bar{1}$2}, and prisms {11$\bar{2}$0} and {0001}. The most developed faces are the faces of the second kind of prism {11$\bar{2}$0} (the seed is parallel to the (10$\bar{1}$0) surface) (figure 1).

Beryl $Be_3Al_2Si_6O_{18}:Cr^{3+}$. Single crystals of Cr^{3+}-doped beryl (emerald) grown under hydrothermal conditions are faceted by the faces of the following crystallographic forms: prism {10$\bar{1}$0}, {11$\bar{2}$0}, bipyramid {11$\bar{2}$1}, bipyramid {10$\bar{1}$2}, pinacoid {000$\bar{1}$}; the forms are given in the order of frequency of occurrence. The same faces are often present on the natural crystals. The growth rates in the directions perpendicular to these singular surfaces are very

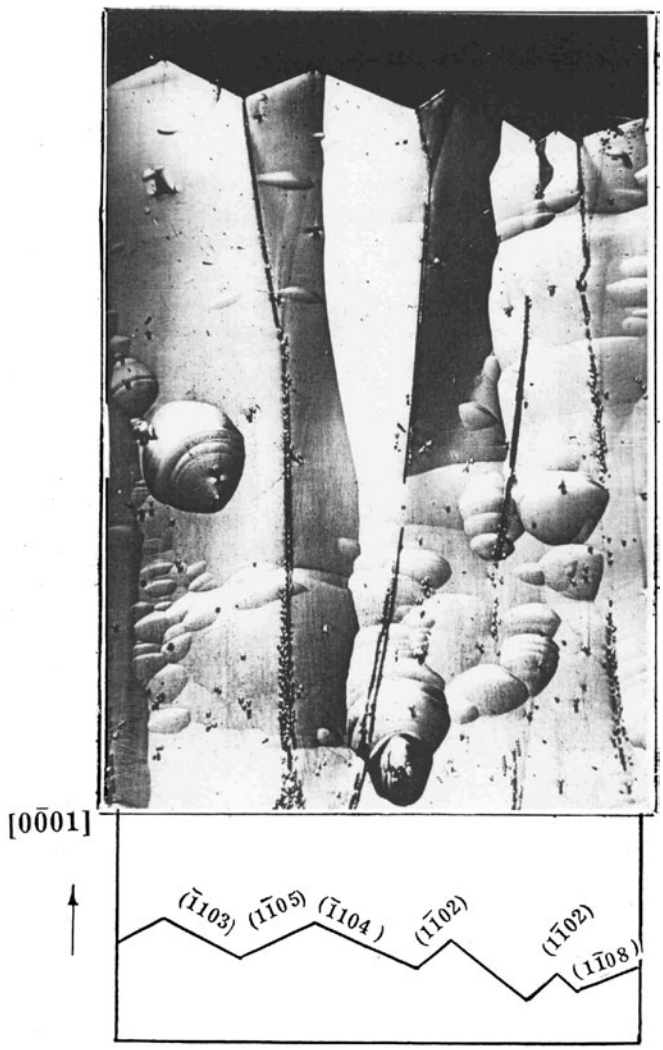

Figure 3. Beryl. Typical growth morphology of the (11$\bar{2}$0) face (×35). The broken line corresponds to the intersection of the prism face with the surface of regeneration.

low and special orientations of regeneration growth have been chosen for growing bulk crystals. The seed surfaces were normal to the face of the first kind of prism {10$\bar{1}$0} and formed the angle 10°–80° with the (0001) surface (figure 2(a)).

When $Be_3Al_2Si_6O_{18}$ crystals are grown on seeds perpendicular to the direction of regeneration growth, their habit is defined by the development of the singular faces which are the closest to the regeneration surface—bipyramids {11$\bar{2}$1}, {10$\bar{1}$2}; prism {11$\bar{2}$0}. The regenerating surface is the base of the pyramid; its apex is the point of intersection of the singular surfaces which are developed onto the regeneration surface (figure 2(b)). The direction of the fastest growth is [11$\bar{2}$1]. Growth in the direction of the regeneration growth occurs due to the growth of the pyramids {1$\bar{1}$0$\bar{2}$}, {$\bar{1}$10$\bar{2}$}, {2$\bar{2}$03}, {1$\bar{1}$0$\bar{5}$}, {$\bar{1}$10$\bar{3}$}, {$\bar{2}$20$\bar{3}$}, {1$\bar{1}$08} (figure 3). The growth rates of the regenerated surfaces were 0.2–0.25 mm/day; the growth rate of the faces of the first kind of prism is more than one order lower (0.01–0.025 mm/day).

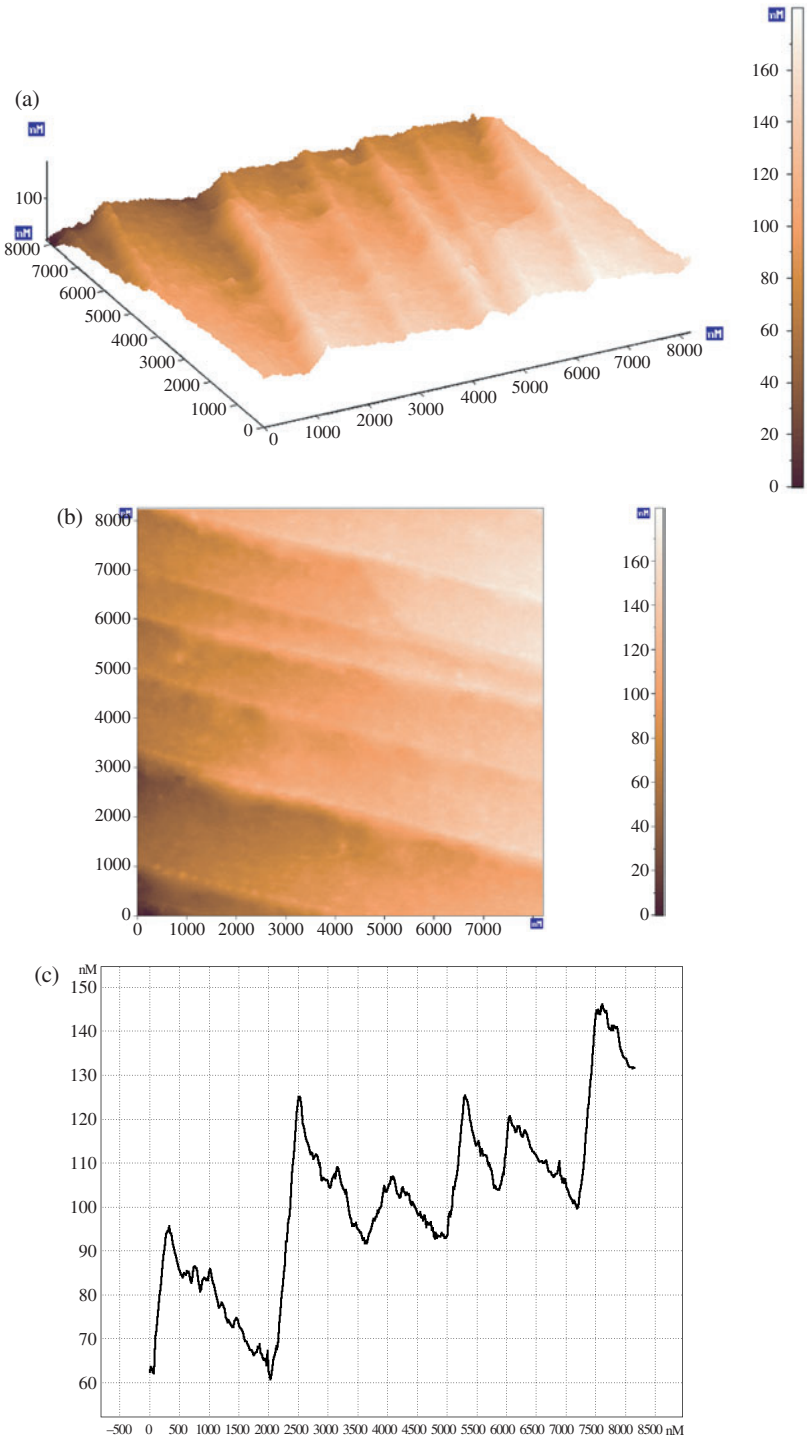

Figure 4. An AFM image of the $(11\bar{2}0)$ face of haematite single crystal, sample f1_1_3. The step propagation occurs in the [0001] direction. (a) Projection onto $(11\bar{2}0)$; the AN line corresponds to the [0001] direction; (b) a three-dimensional image; the step edge is normal to the [0001] direction; (c) a profile of the surface relief along the line with coordinates 3000/0–4500/8000.

Table 2. Typical characteristics of $\{11\bar{2}0\}$ surfaces of haematite single crystals.

Area, $N_x \times N_y$ (nm^2)	8192.4 × 8229.7	3634.8 × 3657.8	3552.6 × 3560.9	1335.3 × 1339.1	615.8 × 614.8	334.4 × 334
R_{max} (nm)	183.8	123.8	26.3	82.6	30.1	8.19
R_{mean} (nm)	105.2	55.0	10.5	15.3[b]	8.83[b]	4.5[b]
R_a (nm)	26.1	18.4	2.69[a]	7.4	3.89	0.91
Sample	f_1_1_3	f_1_1_4	f_1_1_11	f_1_1_3	F_1_1_4	f_2_1_7
D_F(profile)	1.94	1.95			1.94	

[a] Single step.
[b] Rounded growth accessories; D_F(profile)—fractal dimension calculated for the profile line using the method of squares.

3.2. Morphology of the main faces

Haematite Fe_2O_3. The growth surface morphologies have been studied on as-grown crystals without special treatment or etching (only natural etching during autoclave cooling and soft cleaning of the surface with alcohol vapours). At high supersaturation (sufficient or excess mass transfer) the layer-by-layer growth mechanism is characteristic of most developed faces—faces of the $\{11\bar{2}0\}$) prism; these faces demonstrate the typical features of such a growth mode (growth steps). At insufficient mass transfer the transition to skeleton growth occurs and the surfaces assume a specific character with local ruptures between faceted plate-like overgrowing layers.

Macrohatching is typical for the faces of the pinacoid $\{0001\}$ and the $\{11\bar{2}0\}$ prism. On the (0001) face, the overgrown layer is very thin due to the very low growth rate. Some crystals demonstrate a specific hatching which may be explained by twinning with $(01\bar{1}0)$ and $(10\bar{1}2)$ twinning planes. Such twins are located at the angle 120° to one another. The hatching is normal to the edges $(0001)/(11\bar{2}0)$ and parallel to the edges $(0001)/(10\bar{1}0)$. Because the faces of the second kind of prism are the main faces in the habit of grown crystals, let us analyse the micromorphologies of these faces.

The reflection of macrohatching on microscale is a set of large terraces (figures 4(a)–(c)); their horizontal surfaces are parallel to the prism $(11\bar{2}0)$ face, and the vertical sides are parallel to the pinacoid (0001) face. Typical characteristics of $\{11\bar{2}0\}$ surfaces of haematite single crystals are given in table 2. The widths of the terraces are about two orders larger than their heights. Typical dimensions of the terraces (or large flat macrosteps) are 100–150 nm in height and about 10 000 nm in width. Images of terraces at high magnifications have shown that they consist of small steps (height 15–65 nm, width 100–1200 nm). Minimal steps, observed in AFM, have heights of about 2–3 nm at the width of about 10 nm. Notice that the heights of the steps are only a few times larger than the unit cell parameters ($a = 5.03$ Å, $c = 13.75$ Å).

The surfaces of the small steps are not flat; the steps are built from orderly packed rounded globules (figures 5(a)–(c), table 3). The elongation of the globules coincides with $[10\bar{1}0]$ direction. Analysis of the surface by the electron diffraction method has shown that this surface is single crystalline, so the globules cannot be related to deposited polycrystalline material and must be related to the single-crystalline surface.

Under the conditions of insufficient mass transfer, the growth surface presents as elongated globule-like hills on the faces parallel to the c-axis and rounded hills for the (0001) face. The heights of the hills are 0.5–10 nm; the diameter is 10–150 nm. The most often seen size is $h = 0.5$–3 nm, diameter 10–60 nm. Growth occurs due to the mechanism of two-dimensional nucleation. Some characteristics of the surfaces under study are shown in table 3. Very small values of the general roughness R_a indicate the presence of large flat surfaces (terraces).

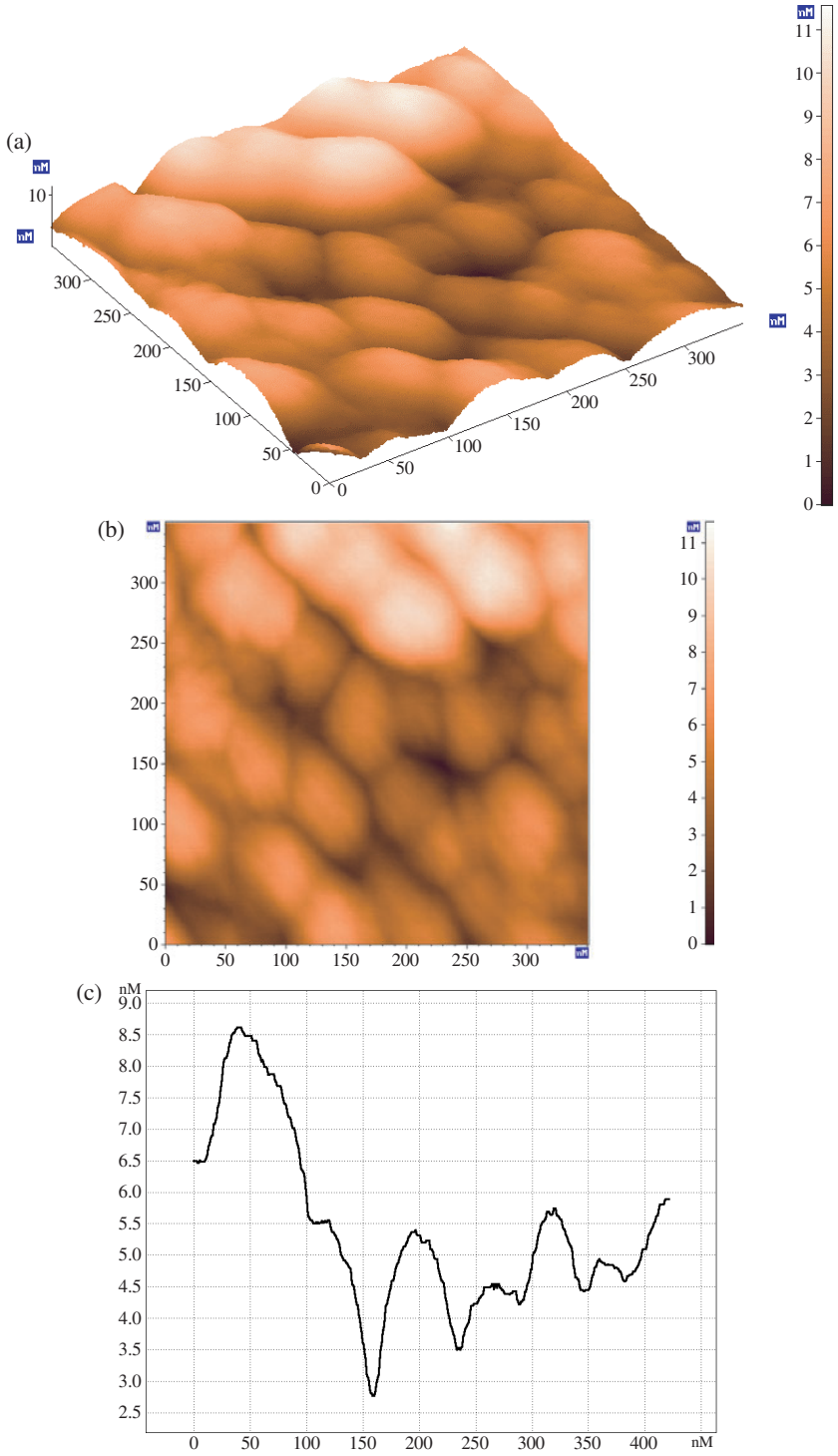

Figure 5. Elongated globules on the $(11\bar{2}0)$ surface of haematite single crystals; sample f1_2_15. The elongation is perpendicular to [0001]. (a) A three-dimensional image; (b) the projection on the plane; (c) the profile along the step propagation direction, along the line with coordinates 0–300/300.

Table 3. Geometrical characteristics of the growth accessories composing the steps on the $(11\bar{2}0)$ surface of haematite single crystals.

Accessories with rounded shape				
Diameter (nm)	0.5–10	<10		1.5–3.5
Sample	f_3_1_3p	f_3_1#5		f_2_1_7
Accessories with oval shape				
Height (nm)	0.6–1.8	0.6–1.5	6–18	0.5–8
Width (nm)	20–35	20	500–900	70
Length (nm)	30–60	50	100–1000	30–130
Sample	f_5_1_3p	f_1_1_9	f_2_2_4	f_1_2_15

The availability of rounded or elongated formations on the surface may serve as an indirect confirmation of the growth mode through rather large clusters or building units consisting of bonded octahedra (ring or chain building units). Note that well-ordered clusters of anisotropic rhombohedra were observed in α-Fe_2O_3 films deposited on α-$Al_2O_3(0001)$ substrate [9]. Those clusters had the heights of about 20–30 Å, and they were preferentially elongated along $[11\bar{2}0]$.

The fractal dimension D_F was calculated for the profile line using the method of squares. The profiles of the crystallization front have the fractal dimension $D_F(\text{profile}) > 1$ (tables 2, 3). The values of D_F are close to 1.9. The results obtained have shown that, in the case of the layer-by-layer growth mode, the morphology of the growing surface may be numerically described in terms of the fractal dimension.

Beryl $Be_3Al_2Si_6O_{18}$. Single crystals were initially etched using etching solvent based on HF. The face $(10\bar{1}0)$ demonstrates the typical features of layer-by-layer growth. Low steps have been found on the prism face (figure 5(a)); their widths are 50–100 nm, their heights 0.5–1 nm (this value is very close to the unit cell parameter values ($a = 9.223$ Å, $c = 9.211$ Å)). The steps arise in the upper part of the seed (usually at the site of seed fixation) and are propagated on the face symmetrically with respect to the seed (projection of the seed surface $\{11\bar{2}n\}$ onto the face $(10\bar{1}0)$). Each step is built of gentle hills with length about 10 nm and width ∼0.4 nm (figure 6(b)). The front of the step propagation is not flat, but zigzag; the dimensions of the ledges/zigzags are about 10 nm.

The data from optical microscopy and goniometry have shown that the regeneration surface is faceted by growth pyramids with the size 0.1–2 mm. These pyramids belong to simple crystallographic forms $\{h\bar{h}0l\}$, $\{h\,h\,\bar{2}h\,l\}$ and are ordered in accordance with the crystallographic orientation of the seed. AFM images demonstrate that these pyramids are composed of cocoon-like hills forming a definite texture on the surface (figure 7). The fills form chains elongated along the direction inclined to $[11\bar{2}0]$ at ∼36° or parallel to the edge of the intersection of the regeneration surface and the $(10\bar{1}0)$ surface. The heights of such hills are 15–70 nm, the widths 100–300 nm.

D_F for the regeneration surface is about 1.7 (table 4). Because the regeneration surface is composed of $\{h\bar{h}0l\}$, $\{h\,h\,\bar{2}h\,l\}$ pyramids, where $l = 2, 3, 5$, at high magnification we will obtain information about the structure of the slope of the hill. As a result, the growth picture will correspond to singular pyramid faces and not to regeneration surfaces. The calculated values of D_F for small mass (high magnification) confirm this (table 4). In this case the values of D_F(profile) will be higher than those for the surfaces with the regeneration growth mode.

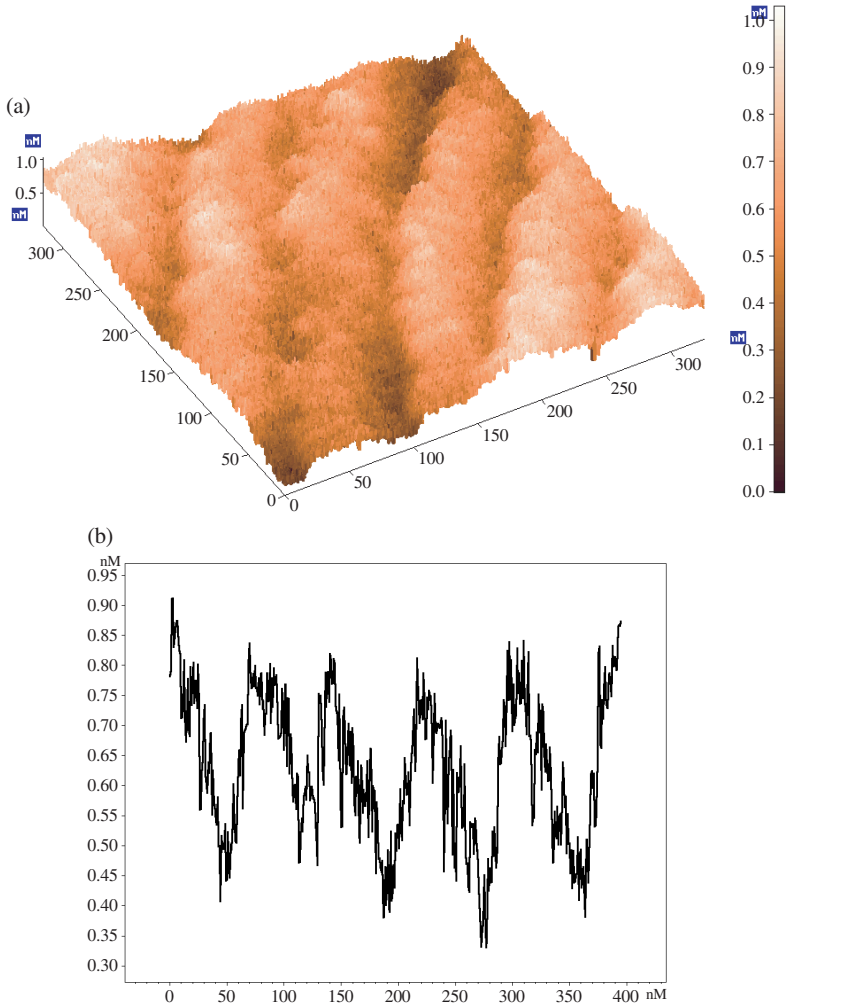

Figure 6. Growth steps on the $(10\bar{1}0)$ surface of emerald single crystal; sample B4_1_18. (a) A three-dimensional image of the growth surface; (b) a profile along the step propagation direction.

Table 4. Characteristics of the regeneration surfaces of beryl single crystals.

Area, $N_x \times N_y$ (nm^2)	4120 × 4130.8	845.5 × 846.6	94.4 × 293.6	292.7 × 292.6
R_{max} (nm)	133.1–116.3	78.8	7.4	9.6
R_{mean} (nm)	74.8–69.7	48.4	4.2	4.2
R_a (nm)	12–14	9	0.7	0.8
Sample	b_1_1_1; b_1_1_6	b_1_1_8	b_1_1_7	b_1_1_7
D_F (profile)	1.74–1.89		1.90–1.96	

3.3. Fractal dimension

We have visualized the morphology of the crystal faces, and obtained and calculated the experimental profiles of the crystallization fronts for haematite and beryl single crystals. At

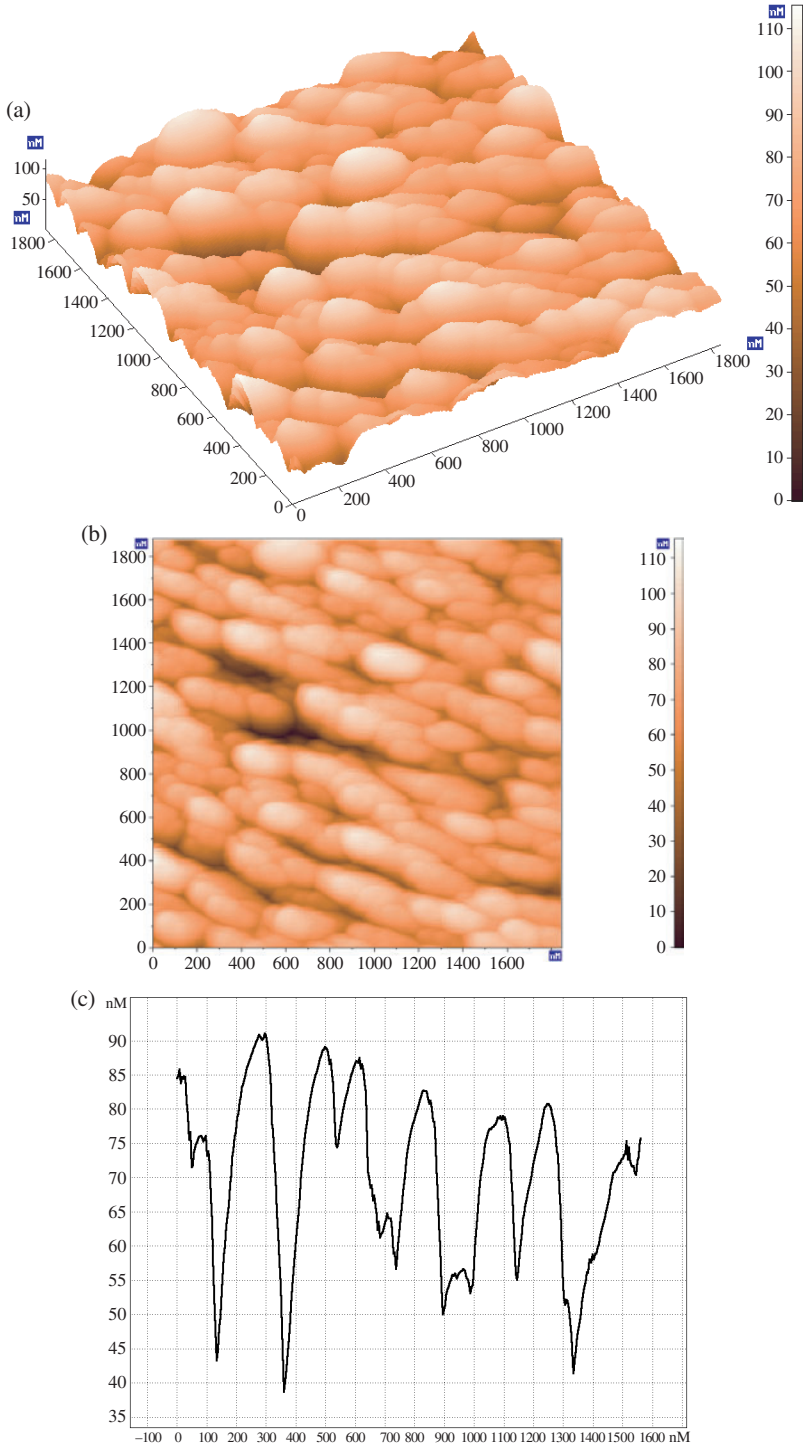

Figure 7. An AFM image of a regeneration surface of beryl single crystal; sample b1-1-7. (a) A three-dimensional image; (b) projection onto the plane; (c) a profile of the surface relief along the direction normal to the elongation of the growth accessories (coordinates 900/0–1500/1400).

the beginning the crystallization front is described as a one-dimensional line (the profile of the crystallization front) although it is a quasi-two-dimensional plane in three-dimensional Euclidean space. The determination of the fractal dimension will allow finding the quantitative relations between the growth rates of various parts of the surface. Thus the crystallization front will be described as a fractal crystallization front if it is represented by a set of simple crystallographic forms or growth accessories (in contrast to a flat, convex, concave crystallization front).

The values obtained for the fractal dimensions for the profiles of crystallization fronts give the first evaluation of the fractal growth mode. More data may be obtained from the analysis of the whole crystal surface. We have evaluated the fractal dimension of the surfaces for the beryl single-crystal surface grown by the regeneration growth mechanism (the area–perimeter method; the fractal dimension has been found for sections with different heights). For the seven samples analysed, we have obtained D_F (surface) equal to 2.6–2.8. These data have shown that the surfaces under investigation have fractal character and may be described using the elements of fractal theory.

4. Conclusions

(1) Single crystals of haematite Fe_2O_3 and a coloured variety of beryl $Be_3Al_2Si_6O_{18}:Cr^3$ (emerald) have been grown on seeds from hydrothermal solutions.
(2) AFM images of the growth morphology for haematite and beryl single crystals have been analysed in the framework of fractal approaches. The results obtained have shown that, in the case of growth on seeds parallel to singular faces and on seeds inclined to the correct crystallographic orientation, the morphology of the growing surface may be numerically described in terms of the fractal dimension.
(3) Minimal steps, observed in AFM on haematite single crystals, have heights of about 2–3 nm at a width of about 10 nm. Geometrically ordered globules compose them. On the nanoscale, the steps demonstrate a geometrically ordered packing of rounded or elongated globules with sizes of 0.5–2 nm. Minimal growth steps on beryl single crystals are characterized by heights less than 0.5 nm.
(4) The availability of rounded and elongated formations on the surface with sizes only several times larger than the unit cell parameters may serve as an indirect confirmation of the growth mode through rather large clusters or building units consisting of bonded polyhedra (ring or chain building units).

Acknowledgment

This work was supported by the Russian Foundation for Basic Research (Grant 03-02-17306).

References

[1] Askhabov A M 1984 *Processes and Mechanisms of Crystallogenesis* (Leningrad: Nauka)
[2] Demianets L N 1996 *17th Congr. and General Assembly of Int. Union of Crystallography (Seattle, WA, USA, Aug. 1996)* PS 16.03 (Collected Abstracts)
[3] Kosova T B and Demianets L N 2000 *Crystallogr. Rep.* **45** 1049
[4] Mandelbrot B B 1977 *Fractals: Form, Change and Dimension* (San Francisco, CA: Freeman)
[5] Rothschhild W G 1998 *Fractals in Chemistry* (New York: Wiley)
[6] Paranajpe A S, Bhakay-Tamhane S and Vasan M B 1989 *Phys. Lett.* A **140** 193
[7] Sawada Y, Dougherry A and Gollub J P 1986 *Phys. Rev.* B **56** 1260
[8] Feder J 1988 *Fractals* (New York: Plenum)
[9] Wang X-G, Shaikhutdinov Sh K, Ritter M, Petersen M, Wagner F, Schögl R and Scheffler M 1998 *Phys. Rev. Lett.* **81** 1038